ARTICLES

Order-disorder transition of ND_4Cl and NH_4Cl

O. H. Seeck,* D. Hupfeld,† H. Krull, M. Tolan, and W. Press
Institut für Experimentelle und Angewandte Physik der Universität Kiel, Leibnizstraße 19, D-24098 Kiel, Germany
(Received 3 November 1997; revised manuscript received 5 February 1998)

ND_4Cl and NH_4Cl single crystals, as model systems for orientational order-disorder phase transitions, were investigated at atmospheric pressure with x-ray diffraction methods. NH_4Cl undergoes a first-order transition whereas for ND_4Cl the transition is very close to a tricritical point (TCP). The order parameter $m(T)$, which describes a low-temperature phase with ferro-ordered NH_4^+ or ND_4^+ tetrahedra, is obtained by analyzing the temperature dependence of the lattice constant a. It is shown that the temperature dependence of a strongly modifies the critical exponent β_{TCP} of the order parameter. In particular, the data yield $\beta_{TCP}=0.16\pm0.01$ in direct neighborhood to the TCP, in good agreement with published values. The departure from the expected mean field value ($\beta_{TCP}=0.25$) is explained by rescaling the critical temperature due to the order-parameter-dependent lattice contraction. For ND_4Cl we got quantitative results for the lattice contraction using a microscopic electrostatic model. Fluctuations related to local antiferro (AF) ordering of the tetrahedra were observed, too. Previously, AF ordering and fluctuations were only observed in NH_4Br and ND_4Br. The correlation length ξ_{AF} of these AF fluctuations exhibits values of 30 Å for NH_4Cl and 10 Å (2–3 lattice constants) for ND_4Cl. [S0163-1829(98)01026-1]

I. INTRODUCTION

Ammonium halides NX_4Y (with X=hydrogen or deuterium and Y=bromine or chlorine) are model systems for Ising-like orientational order-disorder transitions. Below room temperature the generalized phase diagram (see Fig. 1) of the ammonium halides contains three phases: A disordered (D) phase, a ferro (F)-ordered phase with parallel oriented NX_4^+ tetrahedra, and an antiferro (AF)-ordered phase, which only occurs in NX_4Br at not too high hydrostatic pressure. At atmospheric pressure the transitions are of first order with different magnitudes of the discontinuity. At high pressure the discontinuity vanishes and the transitions become second order. The point marking the transition from first order to second order is denoted as the tricritical point (TCP).

In the past, the phase transitions of NX_4Y have been extensively investigated by many authors both, theoretically (see, e.g., Refs. 1–3) and experimentally (see, e.g., Refs. 4–10). Many of these studies focused on the characteristics of the generalized phase diagram. The existence of two differently ordered phases was theoretically explained by Yamada *et al.* and Hüller *et al.* in a semiquantitative manner.[1,11] Though the ammonium halides seem to be well understood, there are still unsolved fundamental problems. The most important is the departure of the measured tricritical exponents from the expected mean field values. For example at the TCP the critical exponent β_{TCP}, which describes the order parameter $m(T)$ near the critical temperature T_c via $m(T)\sim(1-T/T_c)^{\beta_{TCP}}$, is predicted to be $\beta_{TCP}=0.25$. However, values within the interval $\beta_{TCP}=0.15-0.18$ were found for ND_4Cl and pressures between 0 bar and the tricritical pressure $p_{TCP}=(150\pm15)$ bar. A straightforward explanation of the difference was done in the literature by logarithmic corrections of the form $\ln^{1/4}|1-T/T_c|$.[12,13] However, this effect strongly depends on the region $\tau=1-T/T_c$, which is chosen for the data analysis. Close to T_c the logarithmic corrections should be negligible. Hence, $\beta_{TCP}=0.25$ would be still expected. Logarithmic corrections as the only source for the observed β_{TCP} values can be ruled out by our data. Another possible explanation for the unexpected β_{TCP} value could be that the TCP in fact is a multicritical point of higher order. This seems to be unlikely for NX_4Cl,[14] because only two ordered phases are known for the ammonium halides (the aforementioned F and AF phases), that only can lead to a TCP.

In this paper, we suggest that the source of the discrep-

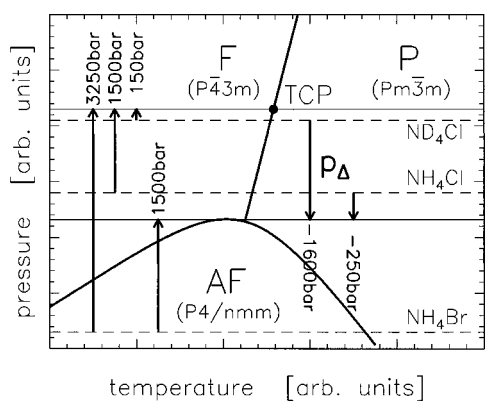

FIG. 1. The generalized phase diagram for ammonium halides. The thick solid lines mark the phase lines, which separate the disordered (D), the ferro-ordered (F), and the antiferro-ordered (AF) phase. The dashed lines denote the atmospheric pressure line for each material. The arrows on the left side are the respective absolute pressure distances between the phases.

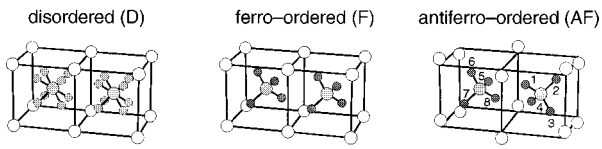

FIG. 2. Microscopic structure of the D phase (space group $Pm\bar{3}m$, left), the F phase (space group $P\bar{4}3m$, middle), and the AF phase (space group $P4/nmm$, right). The light gray spheres at the edges of the cubes mark the halide ions; in the center is the nitrogen atom. The dark spheres are the hydrogen atoms. In the image of the AF phase the H/D positions are identified by the numbers 1–8 (see text). Note that the shifts of the halide ions are exaggerated (in reality it is only 3% of the lattice parameter).

ancy of β_{TCP} from the mean field value is the coupling of the order parameter to the lattice constant. To show this we use a microscopic theory based on previously published work.[1,11] Though only measurements and calculations for the special model system ND_4Cl are presented, the results may be extended to other systems, which show discrepancies between expected and observed tricritical behavior.

Another open question is, if the competing interactions[2] in NX_4Cl crystals lead to fluctuations of an AF-ordered phase. They may occur in the disordered as well as in the F-ordered phase. First indications of AF fluctuations in NH_4Cl were published by Couzi *et al.*[15] Our synchrotron x-ray measurements clearly prove the presence of AF fluctuations in ND_4Cl and NH_4Cl which were recorded over a wide temperature range for the two materials.

II. GENERAL ASPECTS OF NX_4Y

At room temperature ammonium halides NX_4Y crystallize in a simple cubic CsCl structure with the tetrahedral NX_4^+ molecules in the center and the halide ions at the corners of the unit cell. Two nonequivalent orientations of the tetrahedra are possible, which can be identified with a spin-up (↑) and spin-down (↓) state. At room temperature the NX_4^+ tetrahedra are flipping independently.[10] The resulting structure (space group $Pm\bar{3}m$) corresponds to a D phase (see Fig. 2, left).

The tetrahedral arrangement of the hydrogen atoms around the central nitrogen atom yields an octupole momentum as lowest order element of a multipole expansion. The direct octupole-octupole interaction W_{ij} between two NX_4^+ tetrahedra depends on both, the orientation and the distance r. As will be shown later, W_{ij} follows a $1/r^7$ power law, which favors a ferro-ordering of the NX_4^+ molecules. The F-ordered phase remains simple cubic but the point-group symmetry is reduced by a factor of 2 (space group $P\bar{4}3m$, see Fig. 2, center). The order parameter m of the F phase is defined by

$$m=\frac{N_\uparrow-N_\downarrow}{N_\uparrow+N_\downarrow}, \tag{1}$$

with $N_\uparrow$ the number of spin-up orientations and $N_\downarrow$ those with spin down.

Additionally an AF phase is observed in NX_4Br. For a stabilization of the AF arrangement it is necessary to displace the bromide ions by a value Δz along the c axis alternately in positive and negative direction. The resulting change of the internal energy is $W_2\sim\Delta z/r^5$.[16] The displacement of the bromide ions in conjunction with the AF ordering of the NX_4^+ tetrahedra leads to a tetragonal unit cell (space group $P4/nmm$; see Fig. 2, right).

The existence of two different ordered phases can be explained by introducing competing interactions.[11] Roughly speaking, large values of Δz together with large lattice constants a favor the AF phase. Δz is restricted by the hard cores of the electron shells of the halide ions and by the polarizability $\alpha_{p,\mathrm{ion}^-}$,[17] the lattice constant is determined by the radius of the Cl^- or Br^- ion.[18] Because of the higher polarizability and the larger radius of the Br^- ion, the AF phase is preferred in NX_4Br at atmospheric pressure. Decreasing the lattice constant by applying a hydrostatic pressure of about 1500 bar the AF phase vanishes and a transition to the F phase or the D phase is observed[1] (see Fig. 1).

For all ammonium halides a TCP is reached by applying hydrostatic pressure. This common feature opens the possibility to draw a generalized phase diagram, with different atmospheric pressure lines for different NX_4Y compounds (see Fig. 1). To reach the TCP a pressure of 3250 bar is needed for NH_4Br, 1500 bar for NH_4Cl and only 150 bar for ND_4Cl.[7,13,19] These values can be used to determine the distance p_Δ from the atmospheric pressure lines of the ammonium chlorides NX_4Cl to the AF phase (see Fig. 1).

In accordance with the fact that long-range AF order is not observed in NX_4Cl, p_Δ is negative. The generalized phase diagram in Fig. 1 yields $p_\Delta\approx-250$ bar for NH_4Cl and $p_\Delta\approx-1600$ bar for ND_4Cl near the transition temperatures. Thus, at atmospheric pressure NH_4Cl is expected to be in the direct neighborhood of the AF phase and strong AF fluctuations may appear close to T_c. In contrast, ND_4Cl is expected to show considerably weaker AF fluctuations.

It should be mentioned, that the AF fluctuations in NX_4Cl are noncritical and do not yield the critical exponents γ and ν of the susceptibility and the correlation length, respectively. They only can be observed by investigating the F-ordered fluctuations.

III. MICROSCOPIC THEORY

In the previous section qualitative arguments for the existence of two differently ordered phases in ammonium halides were given. The key point is that a direct octupole-octupole interaction between the NX_4^+ tetrahedra favors an F phase, whereas an indirect coupling (via a displacement of the halide ions) leads to the AF phase. A microscopic theory of the latter was given by Yamada *et al.*[1] and Hüller *et al.*[11] Not considered yet is a coupling of the order parameter with the lattice.

In what follows it will be discussed how the critical behavior is altered by a coupling of the order parameter with the lattice of the crystal. We start with a simple qualitative argument based on an interaction energy W_{ij}, that depends on the distance r between the particles i and j in the material. This energy is responsible for the ordering process and is assumed to have the form $W_{ij}(r)=c_{ij}/r^n$. The average over the crystal, i.e., $W=\langle W_{ij}\rangle$, is obviously temperature dependent: W vanishes in the disordered phase because all

the c_{ij} compensate each other. In the ordered phase a dependence on the temperature (thus on the order parameter $m[T]$) is seen, i.e., $W(r,m[T])=C(m[T])/r^n$. This potential has to be added to the common crystal potential $E(r)$ of the disordered phase, which may be in the simplest case a van der Waals or an ionic one. The complete crystal potential now is a function of $m(T)$. This results in a coupling of the order parameter with the equilibrium lattice constant given by $E(r)$ and $W(r,m[T])$. The coupling has in general a remarkable effect on the phase transition. As $W(r)$ is no longer independent of the temperature, and thus on $m(T)$, a modified critical behavior is expected. The effect depends on the actual form of W and $m(T)$. After this qualitative treatment now a quantitative consideration follows for the special case of ND_4Cl where it will be shown that the abovementioned coupling is not negligible and leads to a modified critical behavior.

To calculate the coupling of $m(T)$ to the lattice constant $a(T)$ the interactions between the halide and the NX_4^+ ions have to be considered in more detail. We restrict ourselves to electrostatic interactions. Therefore the charge density distribution $\varrho_{NX_4^+}(\mathbf{r})$ of an NX_4^+ group has to be taken into account. It is a combination of the shell with ten electrons, which can be written as an expansion of spherical harmonics,[20] and the nuclei of hydrogen and nitrogen atoms, which are approximated by δ functions. The positions of the δ functions and the expansion coefficients depend on the orientation of the NX_4^+ molecules and thus on the order parameter $m(T)$.

The interaction energy W_{mn} between two charge density distributions $\varrho_m(\mathbf{r})$ and $\varrho_n(\mathbf{r})$ is given by $W_{mn}=\int U_m(\mathbf{r})\varrho_n(\mathbf{r})d^3r$ with the potential $U_m(\mathbf{r})=\int \varrho_m(\mathbf{r}')/|\mathbf{r}-\mathbf{r}'|d^3r'$. In most cases the exact electron density ϱ_m is too complex for further calculations. Thus approximations have to be found which take into account the symmetry of the molecules and the basic characteristics of the interactions while neglecting details which are expected to be of minor importance for the phase transition. Here the density $\varrho_{NX_4^+,e^-}(\mathbf{r})$ of the NX_4^+ group with its ten electrons was simplified by introducing five different shells, each with spherical symmetry, at the positions of the nuclei. In our approximation the sphere around the nitrogen atom is built up by seven electrons. This means, that only three electrons are left for four ''hydrogen shells.'' Hence each single hydrogen shell contains $\frac{3}{4}$ of an electron, because the time average of the electron density has to be considered, rather than actual locations of single electrons. In calculating W_{mn} it may be easily verified, that it is equivalent to use δ functions instead of the shells with spherical symmetry. Thus the electron density is replaced by

$$\varrho_{NX_4^+,e^-}(r)\approx\begin{cases}-7e\,\delta(\mathbf{r})-\dfrac{3}{4}\,e\displaystyle\sum_{n=1}^{4}\delta(\mathbf{r}-\mathbf{R}_n)\ :\text{spin}\uparrow,\\[2ex] -7e\,\delta(\mathbf{r})-\dfrac{3}{4}\,e\displaystyle\sum_{n=5}^{8}\delta(\mathbf{r}-\mathbf{R}_n)\ :\text{spin}\downarrow,\end{cases}\tag{2}$$

for the spin-up ($\uparrow$) and the spin-down ($\downarrow$) orientation of the NX_4^+ molecule, respectively. The positions of $\mathbf{R}_n$ with $n=1$–8 are shown in Fig. 2; the mean value of $|\mathbf{R}_n|$ is the distance $N\leftrightarrow X$. The value of $N\leftrightarrow D$ is expected to be slightly less than $N\leftrightarrow H$. Within error neutron diffraction measurements reveal $R_n=(1.030\pm0.005)$ Å for both deuterium and hydrogen.[21]

Of course the simplification of the electron density is connected with an error in the further calculations. This error is difficult to estimate. However, as shown below, the model is able to explain our data within the experimental errors indicating that the assumption of the electron density given by Eq. (2) is quite reasonable.

The contribution to the charge density from the nuclei $\varrho_{NX_4^+,\text{nuc}}(\mathbf{r})$ may be calculated similarly to Eq. (2). Thus the total charge density $\varrho_{NX_4^+}(\mathbf{r})=\varrho_{NX_4^+,\text{nuc}}(\mathbf{r})+\varrho_{NX_4^+,e^-}(\mathbf{r})$ is given by

$$\varrho_{NX_4^+}(\mathbf{r})\approx\begin{cases}q\displaystyle\sum_{n=1}^{4}\delta(\mathbf{r}-\mathbf{R}_n)\ :\text{spin}\uparrow,\\[2ex] q\displaystyle\sum_{n=5}^{8}\delta(\mathbf{r}-\mathbf{R}_n)\ :\text{spin}\downarrow,\end{cases}\tag{3}$$

with $q=+e/4$. With this expression one may obtain the interaction energy $W_{TT\pm}$ in terms of multipole-multipole interactions. For two NX_4^+ tetrahedra with parallel ($-$) or antiparallel ($+$) orientation one gets

$$W_{TT\pm}=\frac{4q^2}{\pi\epsilon_0}\frac{1}{a}\left\{1-\frac{7}{9}\left[\frac{R_n}{a}\right]^2+w_\pm\left[\frac{R_n}{a}\right]^6+11\left[\frac{R_n}{a}\right]^8+\mathcal{O}\left(\left[\frac{R_n}{a}\right]^{10}\right)\right\},\tag{4}$$

with $w_-=-\frac{26}{9}$ and $w_+=+\frac{34}{9}$, respectively, and the lattice constant a. For the special case of ND_4Cl, the error neglecting powers of higher order than 10 (the ninth order will not appear) is of about 0.5% of $W_{TT\pm}$. Only the term proportional to $1/a^7$ in Eq. (4), which describes octupole-octupole interactions, depends on the orientation of the tetrahedra. Since the order parameter is defined as $m(T)=(N_\uparrow-N_\downarrow)/(N_\uparrow+N_\downarrow)$ the resulting $m(T)$-dependent part of the interaction energy $W[q,m(T)]$ is a certain combination of W_{TT-} and W_{TT+}. Hence W_{TT-} has to be weighed by a factor $(1+m)/2$ and W_{TT+} by $(1-m)/2$. A detailed calculation including all neighbors of a NX_4^+ tetrahedron yields

$$W[q,m(T)]\approx-61q^2[m(T)]^2\,\frac{R_n^6}{\pi\epsilon_0 a^7}.\tag{5}$$

for the F-ordered phase.[16]

To calculate the coupling of $m(T)$ with the lattice constant $a(T)$ a mean-field-like ionic potential for the disordered phase

$$E(r)=-\frac{e^2\alpha_{\text{CsCl}}}{4\pi\epsilon_0 r}+\frac{C}{r^\nu},\tag{6}$$

is chosen, with the Madelung sum α_{CsCl} and the distance $r=a\sqrt{3}/2$. The exponent ν can be calculated from the bulk

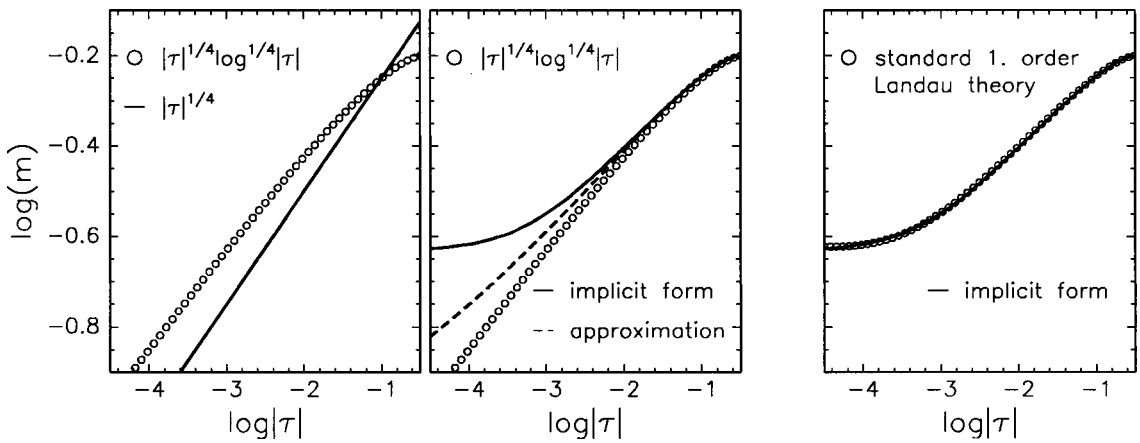

FIG. 3. Log_{10}-$\log_{10}$ representations of the order parameter $m(T)$ for $\beta_{\mathrm{TCP}}=0.25$. In the left part the standard linear model $|\tau|^{1/4}$ is compared with a model that includes logarithmic corrections. In the center image the effect of the rescaled critical temperature T_X is shown. The solid line is based on the implicit form Eq. (9), the dashed line includes the approximation, which is mentioned in the text. The right representation shows that the implicit form of Eq. (9) is almost equivalent to the standard first-order Landau theory.

modulus B and the lattice constant a_0 at the transition temperature.[22] For NX_4Cl the values $\nu=8.47$, $B=17.4$ GPa,[23] and $a_0=3.87$ Å are given. The constant C follows from the condition $(dE/dr)|_{a_0\sqrt{3}/2}=0$. To describe the F-ordered phase the potential given by Eq. (6) is generalized by including the order-parameter-dependent term $W[q,m(T)]$. This leads to $\tilde{E}[r,m(T)]=E(r)+W[q,m(T)]$ and, via minimizing, to a modified equilibrium distance $\tilde{a}(T)=a_0-\Delta a(T)$ with

$$\Delta a(T)=\frac{2562q^2R_n^6a_0[m(T)]^2}{\sqrt{3}e^2(\nu-1)a_0^6\alpha_{\mathrm{CsCl}}-15372q^2[m(T)]^2R_n^6}.$$

For NX_4Cl this can be approximated by

$$\Delta a(T)\approx\frac{2562q^2R_n^6}{\sqrt{3}e^2(\nu-1)a_0^5\alpha_{\mathrm{CsCl}}}[m(T)]^2\approx[m(T)]^2\times 0.01\ \text{Å}. \tag{7}$$

Thus the coupling of the order parameter with the contraction $\Delta a(T)$ is different from the usual linear thermal contraction. In a completely F-ordered state (i.e., $m\equiv 1$) this contraction is expected to be on the order of 0.01 Å compared to the lattice constant of a disordered structure.

Using symmetry arguments Salje[24] found for a transition $Pm\bar{3}m\rightarrow P\bar{4}3m$

$$e_1(T)=[a(T)-a_0(T)]/a_0(T)\sim[m(T)]^2, \tag{8}$$

where e_1 is the only independent component of the cubic spontaneous strain tensor $\underline{\mathbf{e}}$. This result is equivalent to Eq. (7), if the temperature dependence of the D-phase lattice constant $a_0(T)$ is assumed to be weak. For the special case of ND_4Cl this is true $(a_0(T)=[3.808\pm0.002]\ \text{Å}\{1+[5.44\pm0.02]\times10^{-5}\ \mathrm{K}^{-1}\ T\})$.

The maximum value of $\Delta a\approx0.01$ Å for $m\equiv1$ (i.e., $T=0$ K) corresponds to a change of 1.8% for the interaction energy $W[q,m(T)]$. This has a remarkable effect on the phase transition behavior itself, because $W[q,m(T)]$ increases for $T\rightarrow0$ K and a ''self-amplification'' of the ordering effect may be obtained. Therefore, for ND_4Cl the typical critical behavior of the order parameter $m(T)\sim(1-T/T_c)^{\beta_{\mathrm{TCF}}}$ near T_c is not observed. It is possible to obtain the modified form of $m(T)$ by rescaling T_c: In mean field approximation the critical temperature T_c is proportional to $W[q,m(T)]$; thus for NX_4Cl the rescaled critical temperature T_x may be written as

$$T_x=T_c\left(1-\frac{\Delta a(T)}{a_0}\right)^{-7}\approx T_c(1-\varepsilon[m(T)]^2)^{-7},$$

with $\varepsilon\approx0.01$ Å/3.86 Å≈0.0026 [see Eq. (7)]. Then the order parameter follows

$$m(T)=(1-T/T_x)^{\beta_{\mathrm{TCP}}}\approx\left[1-\frac{T}{T_c}(1-\varepsilon[m(T)]^2)^7\right]^{\beta_{\mathrm{TCP}}}. \tag{9}$$

Equation (9) is an implicit expression for the function $m(T)$, which can in general only be solved numerically. The shape of $m(T)$ is very similar to that of the order parameter given by the standard Landau theory for first-order transitions

$$m(T)\sim\sqrt{1+\sqrt{\frac{T_{c\uparrow}-T}{T_{c\uparrow}-T_{c\downarrow}}}}$$

and $T_{c\uparrow}$ and $T_{c\downarrow}$ being the transition temperatures for increasing and decreasing temperature, respectively.[25] This is illustrated in Fig. 3. At T_c the solution of Eq. (9) is

$$m(T_c)=\varepsilon^{\beta_{\mathrm{TCP}}/(1-2\beta_{\mathrm{TCP}})}$$

In the case of $\beta_{\mathrm{TCP}}=0.25$ the discontinuity of the lattice parameter would be $\Delta a(T_c)\approx1.8\times10^{-4}$ Å for NX_4Cl. A comparison to the first order Landau theory would yield a thermal hysteresis of about $\Delta T=T_{c\uparrow}-T_{c\downarrow}\approx0.043$ K. These two values can hardly be observed in experiments. For our setup the error in determining $\Delta a(T)$ was on the order of 10^{-4} Å and that for the temperature was 0.01 K (see Sec. IV).

The effect of the modified critical behavior close to T_c, which is due to the lattice parameter contraction, may only

be relevant for tricritical behavior (or multicritical of higher order) in most cases. Ordinary Ising-like continuous transitions yield an exponent $\beta=0.325$. For this value, the discontinuity directly at T_c decreases rapidly (in our example, $\Delta a \approx 0.058\times 10^{-4}$ Å). Thus, for ordinary continuous transitions the effect of the order-parameter-dependent lattice parameter change can be neglected.

Instead of introducing the abovementioned small first-order component by directly solving Eq. (9), the discontinuity may be avoided by replacing the term $[m(T)]^2$ by the expected behavior $|\tau|^{2\beta_{\mathrm{TCP}}}$, thus

$$m(T)\approx\left[1-\frac{T}{T_c}\left(1-\varepsilon\left|1-\frac{T}{T_c}\right|^{2\beta_{\mathrm{TCP}}}\right)^7\right]^{\beta_{\mathrm{TCP}}}. \qquad (10)$$

With this approximation the transition remains continuous as it is shown in Fig. 3.

As already mentioned in the Introduction for tricritical transitions additional logarithmic corrections have to be taken into account.[12] They are included by multiplying Eq. (9) or Eq. (10), respectively, with the factor

$$[\ln|1-T/T_x|]^{1/4}. \qquad (11)$$

For the special case of $\beta_{\mathrm{TCP}}=0.25$ the effects of the rescaled critical temperature, the logarithmic corrections, and the first-order components on the critical behavior of $m(T)$ are shown in Fig. 3.

IV. SAMPLES, EXPERIMENTAL SETUP, AND DATA ANALYSIS

Single crystals of NH_4Cl and ND_4Cl were used for the investigations. The NH_4Cl samples were grown by Haussühl, University of Köln, Germany. They are mosaic crystals, consisting of crystallites of about 2500 Å diameter. This information was extracted from the full width at half maxima (FWHM) of Bragg reflections. The angular distribution of the crystallites (mosaicity) is about 0.3°. The ND_4Cl samples are from Brockhouse, Collins, and Garrett, McMaster University, Canada. They are approximately 98% deuterated. The size of the crystallites is about 10 000 Å with a mosaicity of 0.035°. This was again deduced from the width of Bragg reflections.

X-ray scattering methods are used to measure the temperature dependence of the lattice parameter $a(T)$ and the AF fluctuations. The investigations were carried out at triple axis diffractometers. The $a(T)$ data were taken at a rotating anode laboratory source (Siemens XP18) with a position sensitive detector (Braun PSD-50M) and the measurements of the AF fluctuations were done at a synchrotron radiation source (ROEWI at HASYLAB). The samples were mounted in a HV chamber ($p<10^{-8}$ mbar). A He-closed cycle cryostat (Leybold RW4000) with a heating and a PID-temperature controller (Lakeshore 330) were used to adjust the temperature in the range of $T=200-300$ K with an accuracy of $\Delta T=\pm 0.01$ K corresponding to a range of $|\tau| = 10^{-4.3}-10^{-1}$ with the reduced temperature $\tau=(T-T_c)/T_c$.

In general, the order parameter of NX_4Y may be directly observed by measuring the intensity change $I(\mathbf{q},T)$ of Bragg reflections. This is simple for the AF phase of NX_4Br because the ordering mode leads to superlattice reflections.[26] In the high-temperature phase $I(\mathbf{q},T)$ is zero, while in the low-temperature AF phase a dependence $I(\mathbf{q},T)\sim[m(T)]^2$ is found.[27] The information about the AF fluctuations in NX_4Y is also located at the superlattice positions where diffusely scattered intensity can be observed.

In the F phase the size of the unit cell remains unchanged compared to the D phase. The only difference is that the NX_4^+ tetrahedra order, which causes a change in the electron density of the hydrogen shell. Thus, an observation of $m(T)$ via intensity changes of Bragg reflections is almost impossible with x-ray scattering (less then 2% of the peak intensity[28]). However, the coupling of $m(T)$ to the lattice parameter can be observed with high accuracy: The contraction $\Delta a(T)\approx[m(T)]^2\times 0.01$ Å [see Eq. (7)] is equivalent to a maximum shift of 0.27° in the scattering angle ϕ, given by $\lambda\sqrt{h^2+k^2+l^2}=2a\sin(\phi/2)$, depending on the Miller indices h, k, l, and the wavelength λ of the used radiation (for this example $\lambda=1.54056$ Å). The errors in determining the *relative* peak positions were estimated to be 0.002° (the Bragg reflections have a FWHM of about 0.05°). This leads to an accuracy of 10^{-4} Å for the change $\Delta a(T)$ of the lattice parameter $a(T)$. We note here, that the *absolute* values of $a(T)$ are only known with an accuracy of about 0.002 Å. Since only $\Delta a(T)$ is of interest, this is no limitation for the data analysis.

To obtain the positions of the Bragg reflections with high precision the full temperature-dependent data series was taken (about 50–60 scans at different temperatures for one hkl reflection) and modeled with a Gaussian shape for each peak. As free parameters the intensities and positions were refined while taking the same FWHM for each data series.

Fluctuations of the AF phase lead to diffusely scattered intensity at the superlattice peak positions $(h,k/2,l/2)$ of the cubic cell. The observed intensity in $\mathbf{q}$ space may be described by a Lorentzian

$$I_{\mathrm{diff}}\sim(1+q^2\xi_{\mathrm{AF}}^2)^{-1}$$

if one assumes an Ornstein-Zernicke-like behavior. ξ_{AF} is the correlation length of the AF fluctuations,[29] which can be obtained from the angular width by

$$\xi_{\mathrm{AF}}=\frac{\lambda}{\pi\sigma_{\mathrm{FWHM}}\cos(\phi_0/2)}.$$

Here ϕ_0 is the center of mass and σ_{FWHM} is the FWHM of the diffuse peak at the superlattice positions.

V. STUDIES OF THE STRAIN IN ND_4Cl

To investigate the coupling of the order parameter with the lattice constant a system with a continuous phase transition may be chosen. This means universal behavior near T_c in the form of a power law $m(T)\sim|1-T/T_c|^{\beta}=|\tau|^{\beta}$. Deviations from this law can be accounted for particular properties of the system [e.g., the rescaling of the critical temperature in NX_4Cl; see Eq. (9)].

In a first step possible hysteresis effects were checked in NX_4Cl to obtain the remnants of the first-order component in these systems. For both materials the data are shown in Fig. 4. NH_4Cl shows a clear first-order transition with $T_{\uparrow}$

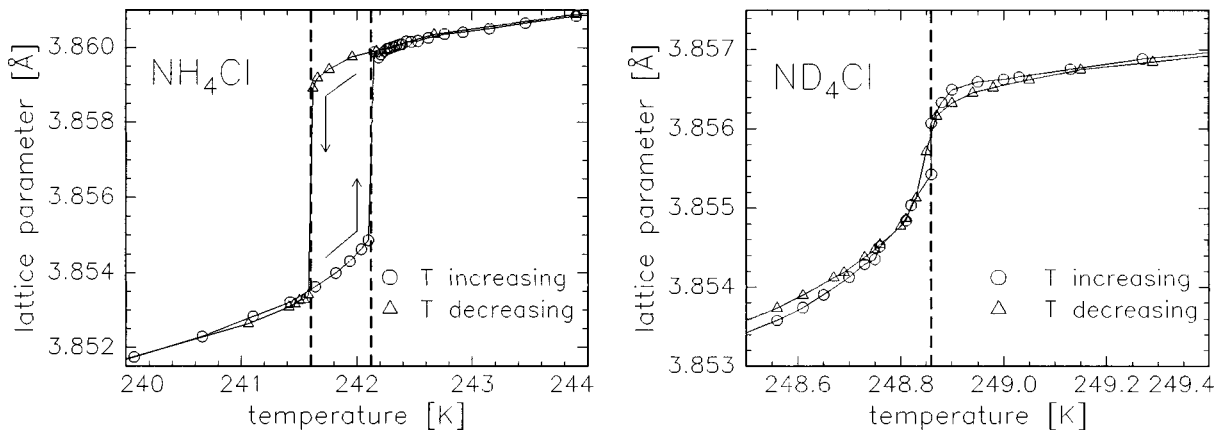

FIG. 4. Measurement (open symbols) of the hysteresis effect in NH_4Cl (left picture) and ND_4Cl. The dashed lines denote the transition temperature. The transition of NH_4Cl is of first order. For ND_4Cl a small first-order component may be seen (open circles at T_c), which depends on the thermal history and cannot be reproduced in each measurement (see open triangles). The lines are only guides to the eyes.

$=(242.13\pm0.20)$ K and $T_{\downarrow}=(241.60\pm0.20)$ K for increasing and decreasing temperature, respectively. This means a thermal hysteresis of $\Delta T=T_{\uparrow}-T_{\downarrow}=(0.53\pm0.04)$ K. The difference between the errors of the absolute values and ΔT are due to the properties of the temperature controller [the accuracy in determining the absolute temperature is only 0.2 K (Ref. 30)]. The first-order component of the transition can also be seen as a jump of the lattice parameter of $\Delta a_{c\uparrow}=(0.0045\pm0.0002)$Å and $\Delta a_{c\downarrow}=(0.0052\pm0.0002)$Å. ND_4Cl shows a different behavior. No hysteresis loop was observed and the transition seems to be continuous with a critical temperature of $T_c=(248.86\pm0.20)$ K (see Fig. 4, right). In some measurements a small jump of the lattice parameter of about $\Delta a_c\approx(0.0005\pm0.0002)$Å appears. This may indicate the direct neighborhood of a tricritical point. Yelon *et al.*[13] and Garland *et al.*[14] got similar results with 93% deuterated samples. They observed a thermal hysteresis of 0.035 K at atmospheric pressure, which vanished at pressures of about 130–150 bar. Therefore ND_4Cl is the system to investigate the tricritical transition and deviations from the expected behaviour because of the change in lattice parameter.

The temperature dependence of the lattice constant of ND_4Cl has been observed for two different samples. We measured the position of the 100, 310, 320, and 311 reflections of one sample with increasing temperature. For the second sample only the 100 reflection was investigated, but for increasing and decreasing temperature to check a possible hysteresis. A typical measurement is depicted in Fig. 5 on a linear scale. It shows the usual linear thermal contraction $a_0(T)=a_{0\,\mathrm{K}}(1+\alpha_{\mathrm{th}}T)$, with $a_{0\,\mathrm{K}}=(3.8076\pm0.0018)$ Å and $\alpha_{\mathrm{th}}=(5.437\pm0.017)\times10^{-5}$ K^{-1} of the disordered phase for $T\rightarrow T_{c,+}$. Below T_c an additional contraction due to the ferro-ordering of the NX_4^+ tetrahedra is observed. It typically saturates for temperatures $T<T_c-20$ K ($|\tau|>0.08$) with a maximum contraction of $\Delta a=(0.0113\pm0.0005)$ Å for ND_4Cl and for NH_4Cl as well. This value is in good agreement with the estimate of $\Delta a\approx0.01$ Å given by Eq. (7). Thus, for NX_4Cl the simple electrostatic model using direct octupole-octupole interactions seems to be the adequate choice for getting quantitative results for the coupling of the order parameter to the lattice.

The reduced lattice constants, which for cubic crystals are equivalent to the component $e_1(\tau)$ of the spontaneous strain tensor $\overline{\mathbf{e}}$ [see Eq. (8)], were used for the logarithmic representation of the data. The double logarithmic plot of $e_1(\tau)$ demonstrates that the data do not follow a simple power law such as

$$e_1(\tau)\sim|\tau|^{2\beta}. \tag{12}$$

Departures are visible in the overall shape of the curves, which are bended for $|\tau|\rightarrow0$ as well as for $|\tau|>0.02$. Both lead to $2\beta=0.22\pm0.02$ instead of the expected value of $2\beta_{\mathrm{TCP}}=0.5$ for a tricritical transition, when using Eq. (12) to fit the data (see Fig. 6). The overall χ^2, which is a measure for the deviation between all fits and the data, was found to be $\chi^2=0.075$. Taking into account logarithmic corrections given by Eq. (11) seem to improve the fit slightly. This leads to $2\beta=0.32\pm0.02$ which is not much closer to $2\beta_{\mathrm{TCP}}$. However, the obtained $\chi^2=0.087$ is even larger but still comparable to the previous value. Hence no significant im-

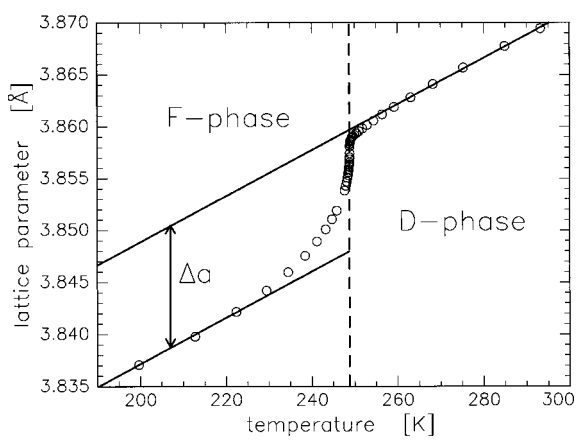

FIG. 5. Temperature dependence of the lattice parameter of ND_4Cl using the 310-Bragg reflection. The dashed line marks T_c, the solid lines mark the linear thermal contraction in the high-temperature phase and the low-temperature phase, respectively. The anomalous contraction $\Delta a(T)$ due to the F ordering can clearly be seen. It saturates below $T<T_c-20$ K at a value of $\Delta a=(0.0113\pm0.0004)$ Å.

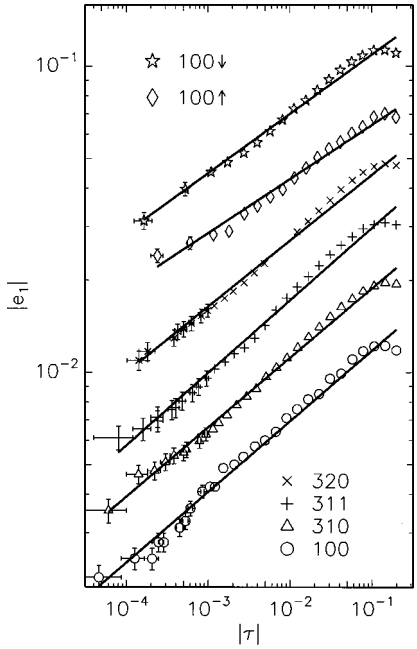

FIG. 6. Temperature-dependent strain obtained from several Bragg reflections of ND_4Cl and a refinement using $|e_1(\tau)| \sim |\tau|^{2\beta}$. For sample 1 the 100, 310, 311, and 320 Bragg reflections were used for increasing temperature, for sample 2 the 100 reflection for increasing and decreasing temperature. It can be seen clearly, that for low temperatures ($|\tau| \to 1$) and for $T \to T_c$ ($|\tau| \to 0$) a simple power-law behavior cannot explain the data. Error bars are only shown if they exceed the symbol size.

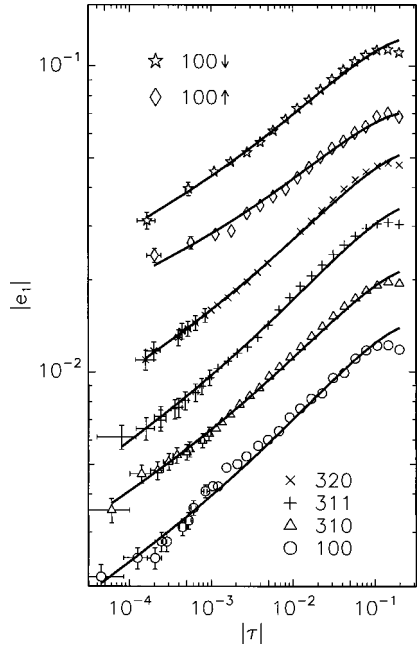

FIG. 7. The temperature-dependent strain of ND_4Cl and a refinement using logarithmic corrections and the approximation Eq. (10), which does not change the continuous character of the transition. This fit yields the best results (see text).

provement is achieved. We also tried to get better fits using a modified form of the logarithmic corrections with an exponent β instead of $\frac{1}{4}$ but without success: the logarithmic corrections mainly influence the curvature far away from T_c and not at the transition itself. In a next step, the data are refined with the model of the rescaled critical temperature T_χ. The best results are yielded by the approximation, that let the transition remain continuous [see Eq. (10)], in connection with the logarithmic corrections (see Fig. 7). The fit reproduces both the bending near T_c and the curvature for $\tau \to 1$. It leads to $\chi^2 = 0.042$, which is two times better than before. For the exponent a value of $2\beta = 0.44 \pm 0.02$ is obtained, which is quite close to $2\beta_{\mathrm{TCP}}$. We also try to refine the data with the implicit form Eq. (9). The fit yields $2\beta = 0.43 \pm 0.03$, but the curvature close to T_c seems to be too large compared to the measurement (see Fig. 8) and the χ^2 only exhibits a value of 0.108.

It should be mentioned that some systematical differences in the measurements were observed, too. Small differences in the up and down temperature cycles are visible and also small differences between the measurements of the two samples do exist (see Figs. 6–8). The former may be due to the fact, that the measurements were not exactly done at the TCP but 150 bar away. Thus a tiny first-order component may remain (as explained above), which may lead to a hysteresis effect. It is very likely that the latter effect may be caused by a slightly different deuteration of the samples. As it can be seen from the generalized phase diagram Fig. 1, the degree of deuteration fixes the normal pressure lines and thus influences the critical behavior. The less the degree of deuteration is, the larger the first-order component would be.

For the analysis all available data were used. This of course leads to relatively large error bars of the above mentioned β_{TCP} values, which are calculated from the β_{TCP} of each curve using statistics. On the other hand, however, the data and the analysis is more reliable and the general effects such as the bending of the curves and the non-mean-field β_{TCP} are more pronounced since they are clearly visible in all measurements.

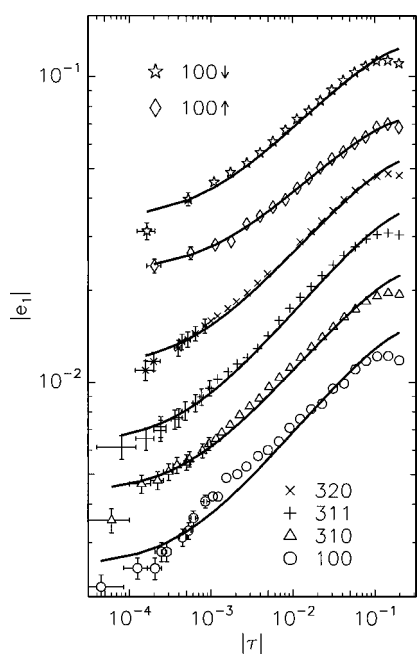

FIG. 8. The data set of ND_4Cl and a refinement using logarithmic corrections and the complete implicit form given by Eq. (9). The predicted first-order jump is somewhat too strong compared with the measurements near T_c, but still agrees within the errors.

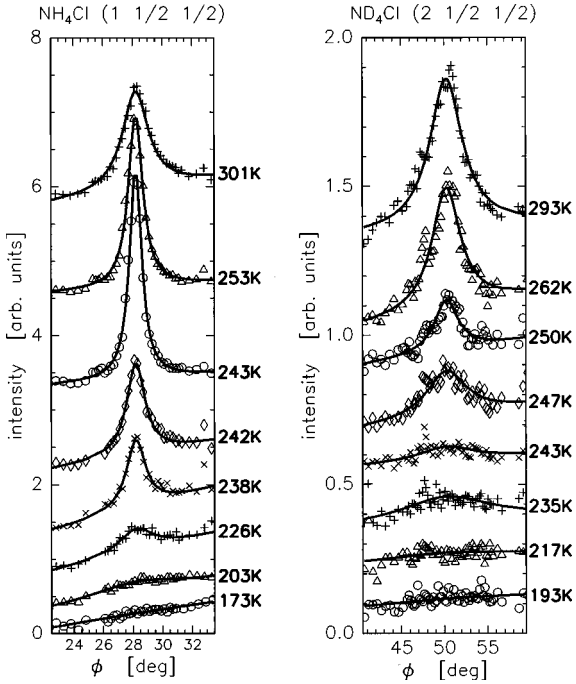

FIG. 9. Detector angle (ϕ) scans at the $(1, \frac{1}{2}, \frac{1}{2})$- and the $(2, \frac{1}{2}, \frac{1}{2})$-superlattice positions of NH_4Cl and ND_4Cl, respectively. In the F-ordered phase (at low temperatures) the AF fluctuations are completely suppressed. At the transition temperature the diffuse scattering exhibits a maximum. The lines represent Lorentzian fits with linear background.

VI. STUDIES OF AF FLUCTUATIONS IN NX_4Cl

As pointed out in Sec. II fluctuations of the AF phase may be visible in NX_4Cl, though these materials show long-range F ordering. The reason for this are competing interactions, which seem to be more relevant in NH_4Cl compared to ND_4Cl (see the generalized phase diagram 1). AF fluctuations are visible as diffusely scattered intensity at the $(h,k/2,l/2)$ superlattice positions, which are at the zone boundary (see Sec. IV).

Figure 9 shows as example a measurement of the intensity at the $(1, \frac{1}{2}, \frac{1}{2})$ position for NH_4Cl as a function of the temperature. The change in the intensity and FWHM of the observed peaks is evident. Near the transition temperature of about $T=242$ K the maximum intensity and smallest FWHM are observed. This corresponds to the maximum of the AF fluctuations and the largest correlation length ξ_{AF}, respectively. Figure 9 also depicts measurements at the $(2, \frac{1}{2}, \frac{1}{2})$ position for ND_4Cl, which show similar characteristics as the NH_4Cl sample.

The AF fluctuations in NX_4Cl were investigated at several superlattice peak positions [NH_4Cl: $(1, \frac{1}{2}, \frac{1}{2})$, $(\frac{3}{2}, \frac{1}{2}, 1)$, and $(2, \frac{1}{2}, \frac{3}{2})$, ND_4Cl: $(2, \frac{1}{2}, \frac{1}{2})$ and $(3, \frac{1}{2}, \frac{1}{2})$] to obtain information about the correlation length ξ_{AF} in different directions of reciprocal space. The deuterated and the hydrogenated samples differ in the surface orientation, mosaicity, and sample size. However, a comparison between the absolute level of the diffusely scattered intensities I_{diff} of the two materials has been done. The corrected integrated intensities of the two materials seem to be comparable within a sizeable uncertainty of the factor of 5–10. More quantitative information cannot be extracted from the intensities because particularly the respective mosaicities are only known very inaccurately.

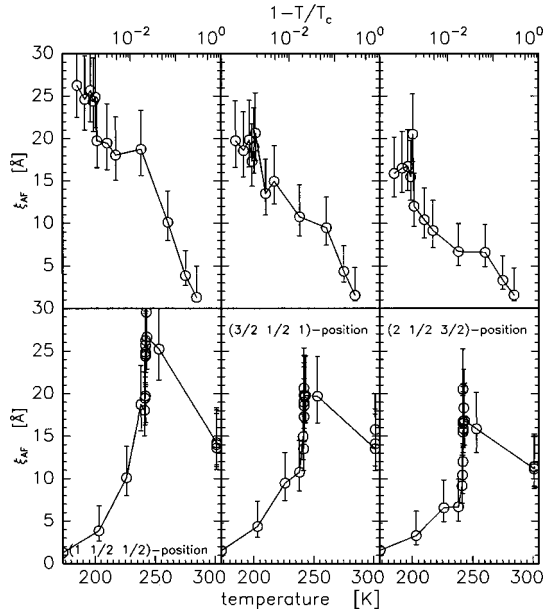

FIG. 10. Correlation lengths of the AF fluctuations in NH_4Cl, measured at three different superlattice positions. The top image shows the log-lin representation for $T<T_c$, the bottom image the whole data on a linear scale. Within the errors the curves are identical. The solid lines are guides to the eyes.

Since the FWHM of the diffusely scattered intensity is independent of the abovementioned differences between the two samples (for $\xi_{AF} \ll$ crystallite size), a quantitative comparison becomes possible. Figures 10 and 11 show the observed values of $\xi_{AF}(T)$ for NH_4Cl and ND_4Cl. For the two samples ξ_{AF} vanishes for $T<200$ K, in accordance with the

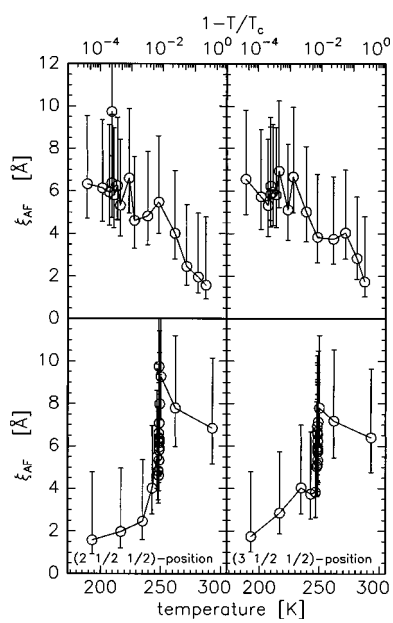

FIG. 11. Log-lin (top) and linear (bottom) representation of the correlation lengths ξ_{AF} of the AF fluctuations in ND_4Cl, measured at two different superlattice positions. Within the errors the curves are identical. The fluctuations are much more suppressed as in NH_4Cl. The solid lines are guides to the eye.

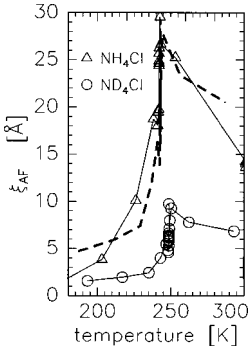

FIG. 12. Comparison of the correlation lengths for NH_4Cl and ND_4Cl. The thick dashed line denotes the data of ND_4Cl scaled by a factor 3 and shifted by 6 K. The solid lines are guides to the eye.

expectation, that the AF fluctuations are strongly suppressed in the long range F-ordered state of NX_4Cl. With increasing temperature ($T<T_c$) the value of ξ_{AF} increases. The maximum is reached at T_c and ξ_{AF} decreases in the D phase. The overall shape is similar to that of the F susceptibility $\chi(\mathbf{q}_F,T)$, but without diverging at T_c.

The diffusely scattered intensity was measured along different directions in reciprocal space (nearly the [100] and the [101] direction for NH_4Cl and the [111] direction for ND_4Cl). Within the error bars ξ_{AF} is independent of the direction, thus indicating almost isotropic fluctuations.

The overall behavior of $\xi_{AF}(T)$ is the same for NH_4Cl and for ND_4Cl. This is demonstrated in Fig. 12 by rescaling the ND_4Cl data with a factor of 3 and shifting the curve by 6 K to the lower transition temperature of NH_4Cl. The main difference between the AF fluctuations in ND_4Cl and NH_4Cl is the magnitude of ξ_{AF}. Due to the direct vicinity of the long-range AF phase (see Fig. 1), we observe strong fluctuations in NH_4Cl and a maximum value of $\xi_{AF}=(30\pm4)$ Å at T_c. With $a\approx3.87$ Å, this is equivalent to the rather large value of $\xi_{AF}\approx7-8$ lattice constants. In contrast to NH_4Cl the ND_4Cl sample only shows weak AF fluctuations. They reach a maximum correlation length of $\xi_{AF}=(10\pm3)$ Å at T_c (2–3 lattice constants). Therefore, AF fluctuations are strongly suppressed in ND_4Cl, as expected from the generalized phase diagram Fig. 1.

To our knowledge, no theory exist that describes the properties of non-order-parameter fluctuations, such as the observed AF fluctuations above, properly. However, in fact the general picture seems to be comparable to the behavior of the order parameter: An increase of the AF fluctuations near T_c, both for $T\rightarrow T_{c,+}$ and for $T\rightarrow T_{c,-}$. However, the AF fluctuations clearly show no singularity at T_c. A comparison with a microscopic theory, as shown in the first part of this paper for the order parameter, would lead to further insight into the microscopic details of the interactions between the molecules of the investigated materials. This has not been done yet.

VII. SUMMARY, CONCLUSIONS, AND OUTLOOK

The phase transition of the ammonium chlorides NH_4Cl and ND_4Cl has been measured with x-ray scattering methods. In the first part the TCP of ND_4Cl was investigated. Very close to the TCP, ND_4Cl seems to exhibit a critical exponent $\beta_{TCP}=0.16-0.18$ instead of the expected mean field value of $\beta_{TCP}=0.25$. This value is in good agreement with previously published data obtained by other methods. The effect of the decreased β_{TCP} is explained by a coupling of the order parameter to the lattice that leads to a ''self-amplifying'' ordering process of the NX_4^+ tetrahedra below T_c. Although we found this explanation for the particular example of NX_4Cl for which a microscopic model is presented one may speculate that this is a more general feature depending on the kind of transition and the special microscopic interactions. The microscopic model includes the direct octupole-octupole interactions between the NX_4^+ tetrahedra and has led to a quantitative description of the measurements for ND_4Cl. In good agreement with the predictions, a lattice contraction of about $\Delta a=0.0113$ Å and a quadratic dependence $\Delta a(T)\sim[m(T)]^2$ has been confirmed. With a rescaled critical temperature T_χ, which depends on $a(T)$, it is possible to explain the difference between β_{TCP} and the expected mean field value. However, T_χ leads to a tiny discontinuity of the temperature dependence of lattice parameter $a(T)$ at T_c.

An alternative approximation which assumes that the phase transition still remains continuous yields even better results. With this assumption an exponent of $\beta_{TCP}=0.22\pm0.01$ is obtained, that is quite close to the expected value. Since the measurements did not take place exactly at the TCP it is not expected to get the precise value of $\beta_{TCP}=0.25$. Of course it is not possible to do an interpolation with only one value of β, which was measured at normal pressure, to obtain an estimation of the real β_{TCP} at $p=150$ bar. But the facts that the corrected value of $\beta=0.22\pm0.01$ is very close to 0.25 and the uncorrected value is close to the previously published values of the uncorrected β_{TCP} indicate that it may reach 0.25 at $p=150$ bar as expected from mean field theory.

Additionally AF fluctuations in NH_4Cl and ND_4Cl have been investigated. The generalized phase diagram shows, that long-range AF ordering does not occur in those materials. Measurements of the diffusely scattered intensity at the superlattice positions yield temperature-dependent short-range AF fluctuations with correlation lengths ξ_{AF} which exhibit values of 30 Å (corresponds to 7–8 lattice constants) for NH_4Cl and, in accordance with the generalized phase diagram, only 10 Å (corresponds to 2–3 lattice constants) for ND_4Cl. The measurements reveal that these AF fluctuations seem to be isotropic.

Future measurements of $a(T)$ with ND_4Cl directly at the TCP, i.e., at $p=150$ bar hydrostatic pressure, would be of great interest. Our considerations predict that these measurements yield exactly $\beta_{TCP}=0.25$ but with the rescaled temperature T_χ instead of T_c. Another interesting point would be the investigation of a possible very small first-order component of the phase transition, which in fact would allow a further investigation of the predictions of the given theory.

Furthermore, surface sensitive grazing incidence diffraction measurements were carried out on the ND_4Cl samples to investigate if modified critical behavior with tricritical surface exponents may be detected.[31,32] These results will be published elsewhere.

ACKNOWLEDGMENTS

We would like to express our gratitude to B. N. Brockhouse, M. Collins, and J. Garrett, McMaster University, Canada, for the ND_4Cl samples, and S. Haussühl, University of Köln, Germany, for the NH_4Cl samples. We also thank Th. Brückel and U. Brüggmann for the support at the beamline W1.1 at HASYLAB and A. Hüller, University of Erlangen, Germany for helpful discussions.

*Present address: XFD/Advanced Photon Source, 9700 S. Cass Avenue, Argonne, Illinois 60439-4814.

†Present address: HASYLAB am DESY Notkestraße 85, D-22603 Hamburg, Germany.

[1] Y. Yamada, M. Mori, and Y. Noda, J. Phys. Soc. Jpn. **32**, 1565 (1972).

[2] A. Hüller, Z. Phys. **254**, 456 (1972).

[3] V. G. Vaks and V. E. Schneider, Phys. Status. Solidi A **35**, 61 (1976).

[4] V. Hovi, K. Paavola, and O. Urvas, Ann. Acad. Sci. Fenn. Ser. AI: Math. **6**, 291 (1968).

[5] H. C. Teh, B. N. Brockhouse, and E. R. Cowley (unpublished).

[6] Y. Yamada, Y. Noda, J. D. Axe, and G. Shirane, Phys. Rev. B **9**, 4429 (1974).

[7] W. Press, J. Eckert, D. E. Cox, C. Rotter, and W. Kamitakahara, Phys. Rev. B **14**, 1983 (1976).

[8] M. J. R. Hoch, S. P. McAlister, and M. I. Gordon, J. Phys. C **8**, 53 (1975).

[9] C. W. Garland and J. D. Baloga, Phys. Rev. B **16**, 331 (1977).

[10] J. Töpler, D. R. Richter, and T. Springer, J. Chem. Phys. **69**, 3170 (1978).

[11] A. Hüller and J. W. Kane, J. Chem. Phys. **61**, 3599 (1974).

[12] M. A. Anisimov, E. E. Gorodetskil, and V. M. Zaprudskil, Sov. Phys. Usp. **24**, 57 (1981).

[13] W. B. Yelon, D. E. Cox, P. J. Kortman, and W. B. Daniels, Phys. Rev. B **9**, 4843 (1974).

[14] C. W. Garland, D. E. Bruins, and T. J. Greytak, Phys. Rev. B **12**, 2759 (1975).

[15] M. Couzi, F. Denoyer, and M. Lambert, J. Phys. (France) **35**, 753 (1974).

[16] O. H. Seeck, Ph.D. thesis, Kiel University, 1997.

[17] J. R. Tessmann, A. H. Kahn, and W. Shockley, Phys. Rev. **92**, 890 (1953).

[18] R. D. Shanon, Acta Crystallogr., Sect. A: Cryst. Phys., Diffr., Theor. Gen. Crystallogr. **32**, 751 (1976).

[19] C. W. Garland and B. B. Weiner, Phys. Rev. B **3**, 1634 (1971).

[20] *International Tables for Crystallography*, edited by U. Shmueli (Kluwer Academic, Dordrecht, 1993), Vol. B.

[21] H. A. Levy and S. W. Peterson, J. Am. Chem. Soc. **75**, 1536 (1953).

[22] N. W. Ashcroft and N. D. Mermin, *Solid State Physics* (Saunders, Philadelphia, 1976).

[23] L. Gmelin, *Gmelins Handbuch der Anorganischen Chemie* (Verlag-Chemie, Weinheim, 1950).

[24] E. K. H. Salje, *Phase Transitions in Ferroelastic and Co-elastic Crystals* (Cambridge University Press, Cambridge, 1990).

[25] W. Gebhardt and U. Krey, *Phasenübergänge und Kritische Phänomene* (Vieweg, Braunschweig, 1980).

[26] D. G. Renz, Ph.D. thesis, University Tübingen, 1971.

[27] B. Burandt, Ph.D. thesis, Kiel University, 1993.

[28] O. H. Seeck, W. Press, B. Asmussen, D. Cox, and Q. Zhu (unpublished).

[29] H. E. Stanley, *Introduction to Phase Transitions and Critical Phenomena* (Oxford University Press, Oxford, 1971).

[30] However, this is not of importance since always temperature differences $|T-T_c|$ are observed to determine the critical exponents. For temperature differences the systematical error of 0.2 K cancels and the much smaller error of 0.01 K remains.

[31] H. Dosch, *Critical Phenomena at Surfaces and Interfaces*, Vol. 126 of Springer Tracts in Modern Physics (Springer-Verlag, Berlin, 1992).

[32] B. Burandt, W. Press, and S. Haussühl, Phys. Rev. Lett. **71**, 1188 (1993).